Available online at www.sciencedirect.com
SCIENCE DIRECT®
Advances in Space Research 37 (2006) 38–44
ADVANCES IN SPACE RESEARCH (a COSPAR publication)
www.elsevier.com/locate/asr

Energetic neutral atom imaging mass spectroscopy of the Moon and Mercury environments

Yoichi Kazama [a,*], Stas Barabash [a], Anil Bhardwaj [b,1], Kazushi Asamura [c], Yoshifumi Futaana [a], Mats Holmström [a,2], Rickard Lundin [a], R. Sridharan [b], Peter Wurz [d]

[a] Swedish Institute of Space Physics, Solar System Physics and Space Technology Division, Road E10 Rymdcampus (BOX 812), SE-981 28 Kiruna, Sweden
[b] Space Physics Laboratory, Vikram Sarabhai Space Center, Trivandrum 695022, India
[c] Institute of Space and Astronautical Science, Japan Aerospace and Exploration Agency, Sagamihara, Kanagawa 229-8510, Japan
[d] University of Bern, CH-3012 Bern, Switzerland

Received 29 October 2004; received in revised form 6 May 2005; accepted 6 May 2005

Abstract

Low-energy neutral atom (LENA) imaging is an important technique for doing planetary sciences at magnetized and unmagnetized planets. In the case of the Moon, the precipitating solar-wind causes sputtering, which releases surface atoms as LENAs into space. Moreover, the solar-wind ions may be back-scattered from the surface into space as neutral atoms. At Mercury, in addition to the above processes, LENAs are also generated by the charge-exchange of energetic ions with the exospheric gasses. Global LENA mass spectroscopic imagery at the Moon and at Mercury provides us information on their surfaces and the interaction processes between energetic particles and the surfaces via remote-sensing using LENAs. We are developing a state-of-the-art LENA instrument for the Indian lunar exploration mission Chandrayaan-1 and the Mercury exploration mission BepiColombo. The instrument is light-weight and capable of mass discrimination, including heavy components such as iron, and has high sensitivity to fulfill various scientific objectives in the area of planetary sciences.

Keywords: ENA; Mercury; Moon; Spectroscopy; BepiColombo; Chandrayaan-1

1. Production of low-energy neutral atoms

1.1. LENAs at Mercury

The Mercury environment is a closely coupled system, in which three components interact with each other: the surface, the exosphere and the magnetosphere (Killen and Ip, 1999). As a result of the dynamics of the magnetosphere, the magnetospheric and solar-wind ions precipitate onto the Mercury surface, resulting in atom and ion sputtering (Killen et al., 2001; Massetti et al., 2003; Lammer et al., 2003). The sputtered particles from the surface and photoionized particles from the exosphere are fed into the magnetosphere, affecting its dynamics. Low-energy neutral atom (LENA) imaging is instrumental in understanding the relationship between these three main domains. In this paper, LENAs are defined as neutral atoms having energy much higher than the escape energy (~5 eV for Fe at Mercury) and

* Corresponding author. Tel.: +46 980 79103; fax: +46 980 79050.
E-mail address: yoichi@irf.se (Y. Kazama).
[1] Present address: NASA Marshall Space Flight Center, NSSTC/XD12, Huntsville, AL 35805, USA.
[2] Present address: NASA Goddard Space Flight Center, Greenbelt, MD 20771, USA.

0273-1177/$30
doi:10.1016/j.asr.2005.05.047

up to energies of about 1 keV. LENAs can propagate through interplanetary space carrying with them the information about their parent components and the process which produced them (Wurz, 2000). LENAs at Mercury are produced by: (1) charge-exchange of energetic ions in the near-planet environment with exospheric gasses; (2) sputtering of surface materials; (3) back-scattering of energetic particles precipitating on the surface.

Mercury has a tenuous atmosphere, an exosphere, yet it is sufficiently dense to convert ions of solar-wind and planetary origins into LENAs by charge-exchange, with generated LENA fluxes high enough for reliable detection and imaging (Lundin et al., 1997; Barabash et al., 2001; Orsini et al., 2001). LENA imaging of the Mercury magnetosphere is similar to the neutral atom imaging performed at the Earth (e.g., Mitchell et al., 2001; Pollock et al., 2001). A unique feature of the Mercury magnetosphere is its large temporal variability, which gives rise to pulsating LENA emissions (ENA 'flashes') with a period of minutes (Lundin et al., 1997). It is also expected that LENA imaging enables us to observe the shape of the magnetosphere (Barabash et al., 2001), because charged particles can fill up the entire dayside magnetosphere due to the relatively small size of the magnetosphere. As mentioned above, charge-exchange LENAs can give us information on the global distributions of solar-wind and planetary ions in the Mercury magnetosphere. Remote-sensing of the planetary ions provides a possibility to understand the role of planetary ions in magnetospheric dynamics, such as substorm triggering mechanisms.

The energetic ions coming directly from the solar-wind and the magnetotail, as well as energized planetary ions, may precipitate onto the Mercury surface, resulting in extensive sputtering (Grande, 1997; Lukyanov et al., 2004). The integrated energy spectrum of the sputtered products falls off as E^{-2}, as described by the Thompson–Sigmund formula (Thompson, 1968), and this results in relatively high fluxes of LENAs at energies greater than ~10–100 eV (Massetti et al., 2003; Mura et al., 2005). LENAs originating from the sputtering process can visualize the precipitation regions in a similar way as the terrestrial aurora displays magnetospheric dynamics (ENA 'aurora' at Mercury) (Lukyanov et al., 2004). Measurements of these LENAs are also crucial for understanding the contribution of sputtering to the formation of the Mercury exosphere because it reveals temporal and spatial variations of the sputtering sources.

Another process for the LENA production is the back-scattering of precipitating solar-wind ions from the surface. The flux of the back-scattered hydrogen (which is neutralized on the surface) might be of the order of 10^5–10^6/cm^2 s sr even with a reflection coefficient as low as 0.1–1%, since the flux precipitating onto the surface is large (up to 10^9/cm^2 s sr). Although the energy of the back-scattering hydrogen is lower than the energy of solar-wind protons due to momentum loss, it is still higher than ~100 eV. The back-scattered hydrogen atoms will visualize the precipitation zone of the solar-wind particles.

1.2. LENAs at the Moon

The Moon does not possess a magnetosphere or an atmosphere/exosphere similar to Mercury. LENAs in the Moon environment essentially result from: (1) sputtering of the surface by precipitating energetic ions and (2) back-scattering of solar-wind ions (cf. Bhardwaj et al., 2005).

The flux of LENAs produced by solar photon stimulated desorption (PSD) is negligibly low for energies greater than 10 eV, because of the small momentum carried by photons. Another possibility, micrometeorite vaporization, is also a minor process for >10-eV LENAs on the Moon, because the vaporized surface material has a relatively low temperature of 4000 K (Wurz and Lammer, 2003). Therefore, the sputtering by the solar-wind is the main process which can produce LENAs with energies substantially higher than 10 eV (Futaana et al., 2004), with the exception of back-scattered solar-wind hydrogen.

By measuring Na abundances for different lunar phase angles (the Moon outside and inside Earth's magnetotail), it was established that sputtering is the dominant mechanism in releasing Na atom from the Moon regolith (Potter and Morgan, 1994).

Laboratory experiments made by Elphic et al. (1991) with lunar soil simulants sputtered by 1.5-keV H^+, 4-keV He^+, 5-keV Ne^+, and 5-keV Ar^+ beams showed that secondary ions such as Na^+, Mg^+, Al^+, Si^+, K^+, Ca^+, Ti^+, and Mn^+ were produced. The neutral atom sputtering yield is, however, known to be higher by a factor of 10–100 than the ion yield (Grande, 1997). Thus, most of the sputtered material emerge as neutral species, and these could not be detected in the experiment of Elphic et al. (1991).

One can say that the Moon surface shines in LENAs, which can display particle fluxes impinging onto the surface and reflecting variations in the production of the different atomic species. Thus, LENA imaging can be used to map the elemental compositions of the lunar surface (Futaana et al., 2004).

Magnetic anomalies have been found on the Moon surface (Lin et al., 1998), which create 'mini-magnetospheres' on the Moon, the smallest magnetospheres ever known. The anomalies can stand off the solar wind. This means that in these regions the surface is shielded from precipitating solar-wind ions, and appears as voids in LENA images. Therefore, imaging of sputtered neutrals will provide the shape of such mini-magnetospheres,

which can be used to estimate the magnetic anomaly strength.

2. An ENA instrument for Mercury and lunar missions

2.1. Missions to Mercury and the Moon

We plan to conduct LENA experiments at Mercury and at the Moon with the LENA mass spectrometers onboard an orbiter spacecraft. The Mercury exploration mission, BepiColombo, is now being implemented by the European Space Agency (ESA) and the Institute of Space and Astronautical Science (ISAS) in Japan, and will be launched in 2012. The Indian Space Research Organization (ISRO) is undertaking the lunar exploration mission, Chandrayaan-1, which will be launched in 2007 (cf. Bhardwaj et al., 2005). Our LENA instrument has been selected to fly on both missions, and the development of the instrument is currently ongoing.

2.2. Design driver

The characteristics of sputtered LENAs are defined by microphysics of the particle–surface interactions, which are in principle similar for all celestial bodies. The design requirements can, therefore, be defined for a relatively wide spectrum of objects, which can be studied through LENA measurement. The following design drivers have been applied for the design of the LENA instrument in the optimization and the trade-off study (in order of priority):

- *Instrument weight*. For planetary missions, minimizing the instrument weight has the highest priority. The goal for the instrument weight is 2.0 kg.
- *Wide energy coverage*. Minimum energies of LENAs at high altitudes are expected to be as low as a few eV due to their gravitational binding. On the other hand, charge-exchange LENAs have energies up to a few keV. In order to measure different types of LENAs, a wide energy coverage of ~10 to ~3000 eV is needed.
- *High sensitivity*. The LENA fluxes at high altitudes might be low, which means that a high detection sensitivity should be achieved. According to LENA studies, the instrument should detect LENAs with fluxes down to $\sim 10^4/\mathrm{cm}^2\,\mathrm{s\,sr\,eV}$ taking other limitations into consideration.
- *Mass discrimination*. Sensing the surface composition remotely by measuring sputtered LENAs invoke the need for having a reasonable mass resolution for a LENA instrument. Considering the weight limitation, the mass resolution is sufficient to resolve H, O, Na, K, Fe, which are expected to be abundant at Mercury and the Moon. It may also be noted that a mass coverage from 1 amu (hydrogen) to 56 amu (iron) is needed.
- *High signal-to-noise ratio*. Because low count rates are expected due to low LENA fluxes, the instrument should have a high Signal-to-Noise (S/N) ratio. For a high S/N ratio, a coincidence detection technique, such as a time-of-flight method, is needed.
- *Angular coverage/resolution*. To map sputtered LENAs onto the surface, a wide angular coverage with adequate angular resolution is necessary. The goal is an all-sky coverage with resolutions of ~20–30°. It is possible to scan the field-of-view (FOV) by using the spinning motion or the orbital movement of the spacecraft. Therefore, a fan-shape FOV is a better option.

2.3. Design of the instrument

The ENA sensor consists of four subsystems, namely, a charged-particle rejection system (deflector), a conversion surface, an energy-analysis system (which also performs efficient photon rejection), and a detection system that provides mass (velocity) analysis. Fig. 1 shows the principle of LENA detection.

A neutral particle enters the sensor through the charged-particle rejection system, which rejects ambient charged particles with energies up to ~15 keV by a static electric field. The incoming neutral particle is then positively ionized by hitting a conversion surface and is reflected toward an electric guide of a special shape. Fig. 2 shows a three-dimensional view of the LENA instrument with calculated trajectories of the neutral atoms after ionization on the conversion surface. Fig. 3 illustrates the field of view of the instrument divided into seven sectors.

In the electric guide, the ionized LENA moves along wave-like trajectories ('wave-type' analyzer), while photons are mostly absorbed in UV traps on the walls of the guide. The wave-type electrostatic guide also provides energy analysis. The concept of this guide design is similar to the one used in the MTOF sensor of the CELIAS instrument (Hovestadt et al., 1995) on the SOHO spacecraft, which provides a UV photon rejection factor of 2×10^{-8}.

Since the instrument must be capable of measuring heavy atoms with masses up to 56 (iron), no carbon foils can be used anywhere inside the sensor. Using foils requires post-acceleration by unrealistically high voltages (typically a particle velocity of 1 keV/nuc is needed).

In order to measure the particle velocity (mass), we use the particle reflection method developed for the Neutral Particle Detector (NPD) of the ASPERA-3 and ASPERA-4 experiments onboard ESA's Mars and Venus Express missions (Barabash et al., 2004). After

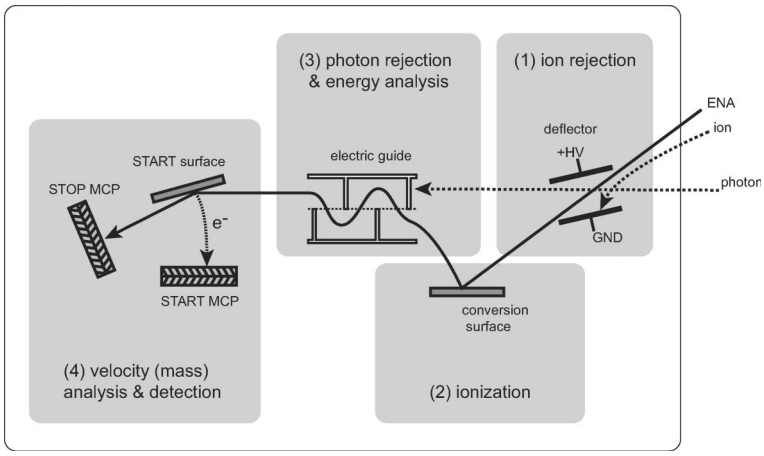

Fig. 1. Schematic diagram for detecting a LENA by the instrument.

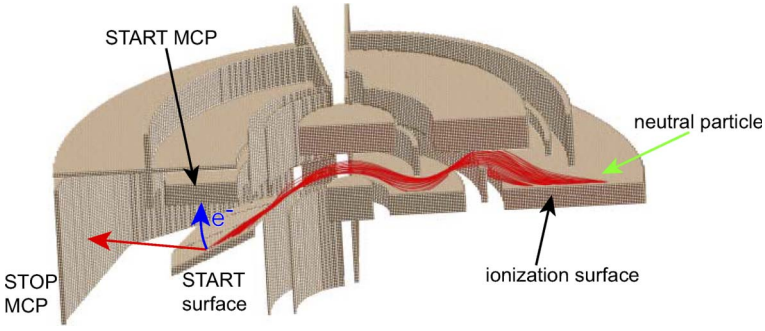

Fig. 2. Three-dimensional cut-away view of the instrument with particle trajectories. Note that the charged-particle deflector is not drawn in the figure.

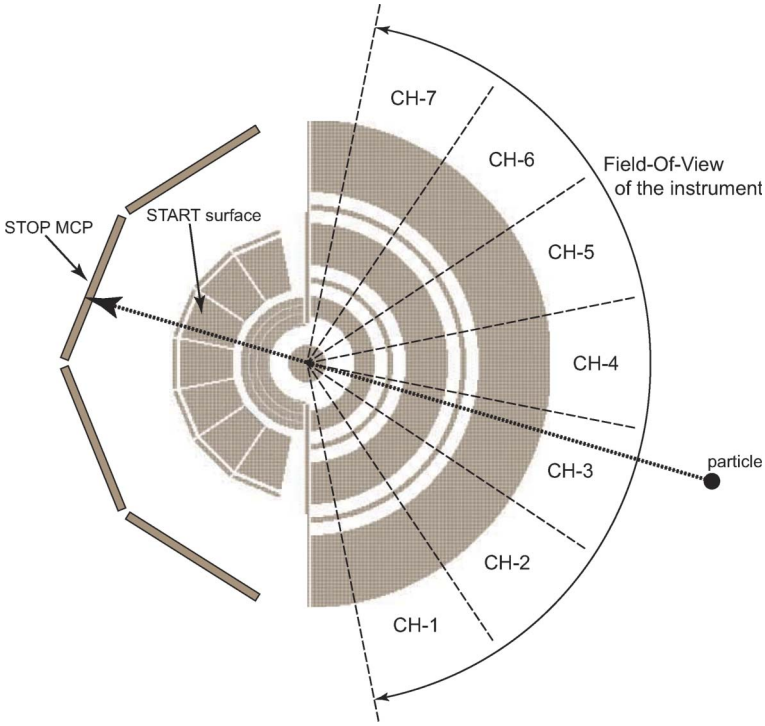

Fig. 3. Azimuthal field of view of the instrument. Seven sectors (CH-1 to CH-7) cover approximately 160° in the azimuthal direction.

exiting the electric guide, the particle is post-accelerated by a voltage of ~3 kV, and impacts on a START surface. Upon particle impact, secondary electrons are emitted from the START surface, which are guided to the START micro-channel plates (MCPs) and produce a START pulse. The example of secondary electron trajectories is illustrated in Fig. 4 with potential contours. The electrons are collected by a small potential difference of 300 V. The START surface, the START MCP, and the post-acceleration electrodes are carefully designed in order not to affect trajectories of incident particles greatly, and we achieved the incident angle, on an average, of approximately 15°. The particle is reflected on the surface towards the STOP MCPs, where it is detected to produce a STOP pulse. The time-of-flight (TOF) between the START and STOP signals gives the particle velocity. Combining the TOF measurement and the energy analysis of the particle, the mass of the LENA particle can be determined.

The START MCP provides the two-dimensional position (in radius and azimuth) and the timing of the particle reflected on the START surface. The radial position allows accurate determination of the TOF length, and the azimuthal position provides the azimuthal angle of the incoming LENA.

We designed this instrument by performing a large number of computer simulations, not only to maximize each performance but also to balance between the priorities listed above. The main difficulty in designing the instrument is the balance between the mass resolution and large geometrical factor, while keeping sufficient angular resolution.

Fig. 5 shows the expected TOF distributions for five major species: H, O, Na, K, Fe. The simulation was done under the condition that the sensor was tuned to an energy of 25 eV, with the energy bandwidth in the electrostatic wave guide and the angular scattering on the START surface taken into account. The mass resolution achieved is sufficient to resolve the main mass groups of LENAs sputtered from the Mercury and lunar surfaces.

As a result of the optimization, sufficiently large geometrical factors are achieved, whose values are ~5 cm^2 sr eV for the 25-eV case and ~50 cm^2 sr eV for the 3300-eV case for each angular sector (channel). Fig. 6 shows the pure (efficiencies are not included) geometrical factors as a function of energy for different sectors (corresponding to different looking directions). The one-count flux level is ~20/cm^2 s sr eV for 25-eV LENAs assuming the overall efficiency ~1%, which is sufficient for Mercury and the Moon.

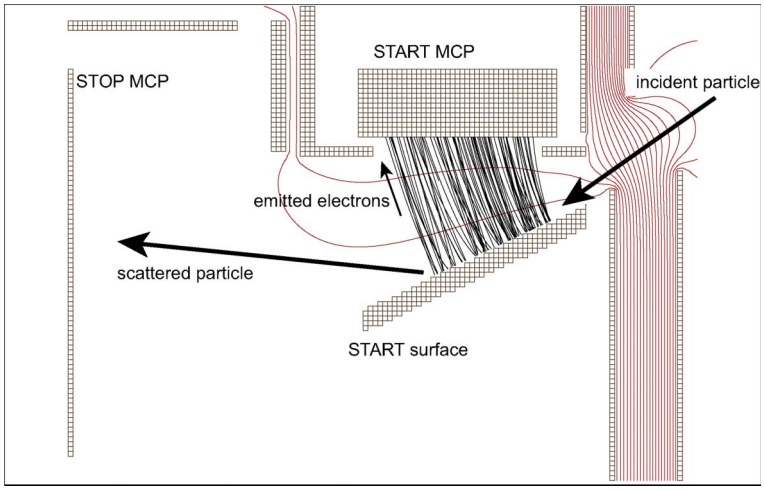

Fig. 4. Trajectories of secondary electrons emitted from the START surface.

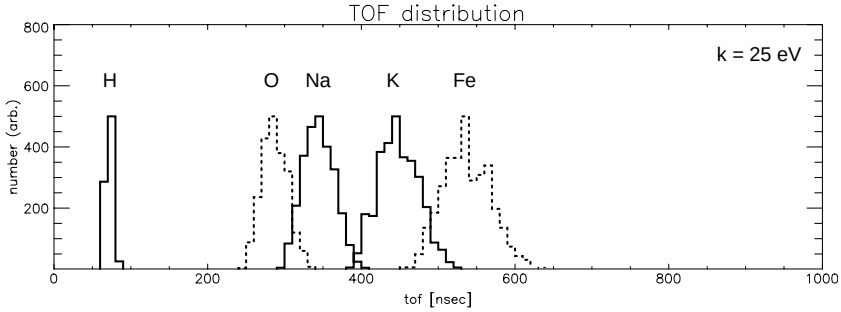

Fig. 5. Time-of-flight distribution for H, O, Na, K, and Fe in the case of the tuned energy k of 25 eV.

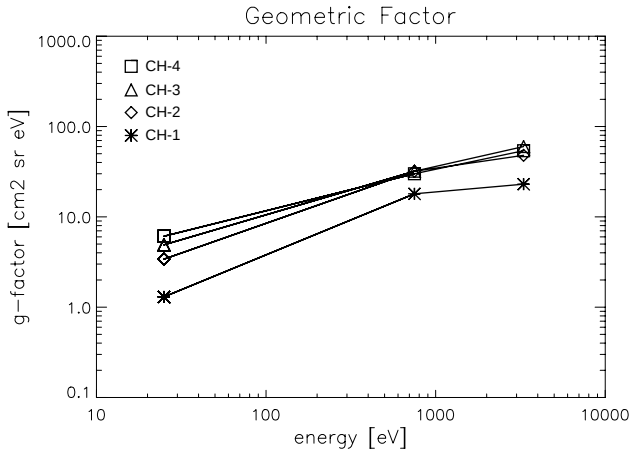

Fig. 6. Pure geometrical factors for each azimuthal channel. Note that channel-5, -6, and -7 are identical to channel-3, -2, and -1, respectively, because of the azimuthal symmetry.

Fig. 7 presents azimuthal angle responses for each sector for 25-eV LENAs. The fields-of-view are approximately 30° in full width at half maximum (FWHM), and the seven sectors cover 160° FOV in the azimuthal direction. The polar FOV is about 9° in FWHM (not shown here), which is defined by the collimator (the electrostatic deflector). Table 1 summarizes the characteristics of the LENA instrument.

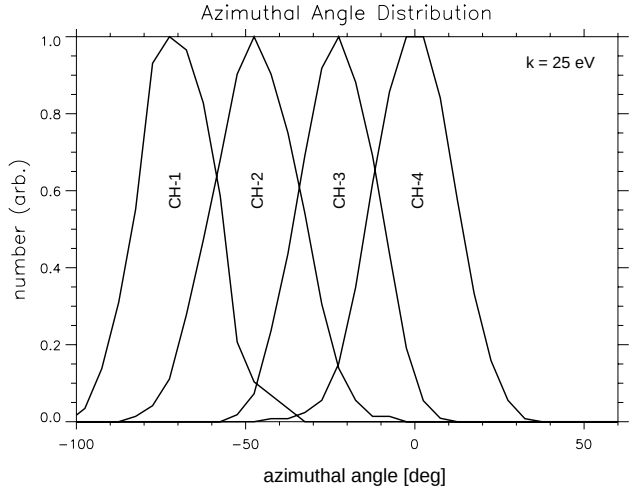

Fig. 7. Azimuthal angle response for each channel in the case of the tuned energy k of 25 eV. Note that channel-5, -6, and -7 are identical to channel-3, -2, and -1, respectively, because of the azimuthal symmetry.

Table 1
Summary of the performance of the LENA instrument

Parameter	Value
Energy range	~10–3300 eV
Geometrical factor	~5 cm^2 sr eV/channel for 25 eV ~50 cm^2 sr eV/channel for 3300 eV
Total efficiency	~1%
Angular resolution	9° × 30°
Field of view	9° × 170° for 25 eV 9° × 130° for 3300 eV
Mass	2.0 kg
Power	3.1 W
Envelope	224 × 207 × 87 mm

3. Summary

LENAs in space are produced by three mechanisms, i.e., charge-exchange, sputtering, and back-scattering processes.

Energetic ions around a celestial body, such as magnetospheric ions and solar-wind ions, can charge-exchange with exospheric gases, and the resulting LENAs continue on ballistic trajectories (mostly straight line). By measuring these LENAs, global distributions and dynamics of ions surrounding the body can be obtained in a way similar as for Earth's ENA imaging.

Energetic particles precipitating onto the surface of the body sputter surface materials, which is called sputtered LENAs. The higher-energy (greater than escape energy) part of the sputtered LENAs can reach high altitudes and can be measured by a LENA instrument on a spacecraft. The sputtered LENAs provides information on how particle precipitation occurs on the surface. In addition, imaging the sputtered LENAs enables us to obtain a map of the surface compositions remotely from orbit.

Back-scattering of precipitating solar-wind particles takes place on the planetary surface and the back-scattered neutrals become LENAs. Measurement of the back-scattered LENAs gives a precipitation map of the solar-wind to the surface of the body.

The latter two processes are universal and can be seen at all non-atmospheric bodies, e.g., the Moon and Mercury. The images of these LENAs can be applied to investigate particle precipitation onto the surface, magnetic field configurations as expected on Mercury, and specific surface properties such as magnetic anomalies on the Moon.

In order to achieve the scientific goals to observe these LENAs as mentioned above, it is important for a LENA instrument to have a wide energy coverage, mass resolution capability, and fine angular resolution. Furthermore, the weight of an instrument is strictly limited for planetary missions.

We have designed a LENA instrument to meet the above requirements. The LENA instrument has a wide energy range from ~10 eV to ~3.3 keV, angular resolution of 9° × 30°, and is capable of resolving major species, such as H, O, Na, K, and Fe. We achieved an overall instrument weight of 2 kg. It should be also noted that the geometrical factor is 5 cm^2 sr eV/channel for 25 eV and 50 cm^2 sr eV/channel for 3300 eV, which is enough to measure tenuous LENA fluxes. The LENA

detection technique employed is based on surface ionization and reflection, which have been well established by other space-borne instruments.

This LENA mass spectrometer has been selected to fly to the Moon onboard the Indian Chandrayaan-1 mission and to Mercury onboard the ESA's BepiColombo mission.

References

Barabash, S., et al. Energetic neutral atom imaging of Mercury magnetosphere 3. Simulated images and instrument requirements. Planet. Space Sci. 49, 1685–1692, 2001.

Barabash, S., et al. The Analyzer of Space Plasmas and Energetic Atoms (ASPERA-3) for the European Mars Express Mission. ESA publication SP-1240, 121–139, 2004.

Bhardwaj, A., et al. Low energy neutral atom imaging on the Moon with the SARA instrument aboard Chandrayaan-1 mission. Earth Planet. Sci.(Proceedings of the Indian Academy of Science), 2005, submitted.

Elphic, R.C., et al. Lunar surface composition and solar wind-induced secondary ion mass spectroscopy. Geophys. Res. Lett. 18, 2165–2168, 1991.

Futaana, Y., et al. Low energy neutral atoms imaging of the Moon. Planet. Space Sci. 2004, submitted.

Grande, M. Investigation of magnetospheric interactions with the Hermean surface. Adv. Space Res. 19 (10), 1609–1614, 1997.

Hovestadt, D., et al. CELIAS – charge, element and isotope analysis system for SOHO. Solar Phys. 162, 441–481, 1995.

Killen, R.M., Ip, W.-H. The surface-bounded atmospheres of Mercury and the Moon. Rev. Geophys. 37, 361–406, 1999.

Killen, R.M., et al. Evidence for space weather at Mercury. J. Geophys. Res. 109, 20509–20525, 2001.

Lammer, H., et al. The variability of Mercury's exosphere by particle and radiation induced surface release processes. Icarus 166 (2), 238–247, 2003.

Lin, R.P., et al. Lunar surface magnetic fields and their interaction with the solar wind: results from lunar prospector. Science 281, 1480–1484, 1998.

Lukyanov, A., et al. Energetic neutral atom imaging at Mercury. Adv. Space Res. 33, 1890–1898, 2004.

Lundin, R., et al. Ion acceleration processes in the Hermean magnetosphere. Adv. Space Res. 19, 1593–1607, 1997.

Massetti, et al. Mapping of the cusp plasma precipitation on the surface of Mercury. Icarus 166, 229–237, 2003.

Mitchell, D.G., et al. Imaging two geomagnetic storms in energetic neutral atoms. Geophys. Res. Lett. 28, 1151–1154, 2001.

Mura, A., et al. Dayside H^+ circulation at Mercury and neutral particle emission. Icarus 175, 305–319, 2005.

Orsini, S., et al. Remote sensing of Mercury's magnetospheric plasma environment via energetic neutral atoms. Plan. Space Sci. 49, 1659–1668, 2001.

Pollock, C.J., et al. First medium energy neutral atom (MENA) images of Earth's magnetosphere during substorm and storm-time. Geophys. Res. Lett. 28, 1147–1150, 2001.

Potter, A.E., Morgan, T.H. Variation of lunar sodium emission intensity with phase angle. Geophys. Res. Lett. 21, 2263–2266, 1994.

Thompson II, M.W. The energy spectrum of ejected atoms during the high energy sputtering of gold. Philos. Mag. 18, 377, 1968.

Wurz, P., Lammer, H. Monte-Carlo simulation of mercury's exosphere. Icarus 164 (1), 1–13, 2003.

Wurz, P. Detection of energetic neutral particles. in: Scherer, K., Fichtner, H., Marsch, E. (Eds.), The Outer Heliosphere: beyond the Planets. Copernicus Gesellschaft, Katlenburg Lindau, pp. 251–288, 2000.